Molecular Ruthenium Cyclopentadienone Bifunctional Catalysts for the Conversion of Sugar Platforms to Hydrogen

Molecular Ruthenium Cyclopentadienone Bifunctional Catalysts for the Conversion of Sugar Platforms to Hydrogen

Alessandro Messori,[a,b] Giulia Martelli,[a,b] Andrea Piazzi,[a,b] Francesco Basile,[a,b] Jacopo De Maron,[a,b] Andrea Fasolini,[a,b,*] Rita Mazzoni[a,b,*]

[a] Department of Industrial Chemistry "Toso Montanari", viale Risorgimento 4, 40136 Bologna, Italy

[b] Center for Chemical Catalysis – C3, University of Bologna, viale Risorgimento 4, 40136 Bologna, Italy.

Corresponding author: **Rita Mazzoni** e-mail: rita.mazzoni@unibo.it; **Andrea Fasolini** e-mail: andrea.fasolini2@unibo.it

Abstract

Molecular ruthenium cyclopentadienone complexes were employed for the first time as pre-catalysts in the homogeneously catalysed Aqueous Phase Reforming (APR) of glucose. Shvo's complex resulted the best pre-catalyst (loading 2 mol%) with H_2 yields up to 28.9% at 150 °C. Studies of the final mixture allowed to identify the catalyst's resting state as a mononuclear dicarbonyl complex in the extracted organic fraction. *In situ* NMR experiments and HPLC analyses on the aqueous fraction gave awareness of the presence of sorbitol, fructose, 5-hydroxymethylfurfural and furfural as final fate or intermediates in the transformations under APR conditions. These results were summarized in a proposed mechanism, with particular emphasis on the steps where hydrogen was obtained as the product. Benzoquinone positively affected the catalyst activation when employed as an equimolar additive.

Introduction

Nowadays the transition toward a hydrogen-based energy system has been pushed forward by different organizations. [1,2,3] However, hydrogen is still mainly produced from fossil fuels and the International Energy Agency reported that in 2021 only 0.2% of the hydrogen energy demand was

produced from renewables (electrolysis or biomass), while methane steam reforming and coal gasification contributed to most of H_2 production.[4]

Though, the production of hydrogen from renewable routes should be addressed for its realistic application as an energy carrier.

Aqueous phase reforming (APR) of polyols and sugars, introduced by Dumesic in early 2000s,[5,6,7,8,9] has allowed to use biomass-derived feedstock, providing some advantages compared to methane steam reforming.[10,11,12,13] In fact, APR has made accessible to work at lower temperatures (250 °C), in liquid phase and at autogenous pressure.[10] Moreover, these reaction conditions are compatible with that of the water gas shift reaction, consuming carbon monoxide and steam raising hydrogen production.[14]

Generally, the APR process can be written as (Eq. 1):

$$C_xH_{2y}O_x + 3H_2O \rightarrow (x+y)H_2 + xCO_2 \qquad (1)$$
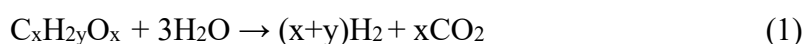
which is the sum of glycerol reforming process (Eq. 2), and subsequent water gas shift process (Eq. 3):

$$C_xH_{2y}O_x \rightarrow yH_2 + xCO \qquad (2)$$

$$CO + H_2O \rightarrow H_2 + CO_2 \qquad (3)$$
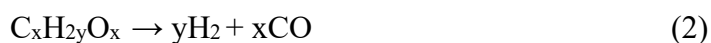
In this framework different polyols and sugars have been used as feedstock for aqueous phase reforming, such as ethylene glycol, glycerol, xylitol, fructose and glucose.[6,8,11,12,15,16,17,18,19] The latter is of particular interest as it can be directly obtained from cellulose by hydrolysis.[20,21,22,23] However, its conversion to hydrogen under the APR conditions is hindered by the production of polymerized side products (humins) above 200°C, which are temperatures usually needed when using metal-based heterogeneous catalysts.[24,25,26] To address this problem, homogeneous catalysis could help the reaction conditions to be milder, whereas different mechanisms could allow better selectivity.[27,28,29,30,31,32,33] For instance, Ru-based homogeneous catalysts has been applied to transfer hydrogenation reactions employing alcohols as substrates.[34,35,36,37,38] Pioneering works carried out by Robinson et al. in the 1970s showed that ethanol dehydrogenation could be accomplished in

systems employing [Ru(OCOCF$_3$)(CO)(PPh$_3$)$_2$] and trifluoroacetic acid in boiling ethanol.[39] Since then, Ru complexes bearing phosphine ligands have been studied for the dehydrogenation of ethanol, glycol and isopropanol.[40,41] Ethanol and isopropanol have been also dehydrogenated using RuCl$_3$·xH$_2$O in the presence of adamantylphosphines or biarylphosphines at lower reaction temperatures.[42] However, the hydrogen production was lower for ethanol as the produced acetaldehyde underwent the Guerbet reaction to give long-chain alcohols.[43,44] The same group then evaluated the activity of a [RuCl$_2$(p-cymene)]$_2$/TMEDA system in isopropanol dehydrogenation,[45] and pincer type complexes have also been applied,[46,47] such as those reported by Beller et al. with a high dehydrogenation activity toward ethanol at low temperatures (100°C) using a non-innocent PNP pincer and [RuH$_2$(CO)(PPh$_3$)$_3$].[48] The same group screened other PNP and PNN pincer ruthenium and iridium catalysts in the reaction of ethanol to ethyl acetate with hydrogen evolution, finding that a high activity could be obtained also with a commercial complex, i.e. Ru-MACHO. However, the addition of a base was needed to carry out the catalytic cycle, pre-activating the catalyst and trapping the acetaldehyde.[49] On the other hand osmium dimers were screened by Gusev et al. and outperformed Ru complexes in ethanol dehydrogenation to ester, being able to work under both basic and neutral conditions.[50,51] They also studied a series of osmium and ruthenium pincer type complexes producing hydrogen and ethyl acetate from ethanol. Glycerol dehydrogenation has also been investigated on Ru ([RuH$_2$(N$_2$)(PPh$_3$)$_3$]) and Rh [Rh(bipy)$_2$]Cl catalysts (Cole-Hamilton 1980), displaying high activity of Rh at 120°C.[52] The activity of the Ru catalyst could be enhanced by three times by irradiation with UV light. Ru-MACHO itself was able to dehydrogenate glycerol at 140°C in N-methylpyrrolidine with the addition of NaOH.[53] Ir catalysts were able to dehydrogenate glycerol to glyceraldehyde, dihydroxyacetone, or even lactic acid at 100-115°C in the absence of a base. In particular, Ir precatalysts with N-heterocylic carbene (NHC) ligands led to hydrogen and lactic acid with 97% selectivity.[54] An even higher TON toward hydrogen and lactic acid production was reported using Ir(I) compounds stabilized by a chelating (pyridyl)carbene ligand.[55,56] Interestingly, the use of the pincer borohydride and formate iron complexes also resulted in lactic

acid production as well as hydrogen evolution at mild conditions (140°C). Increasing the feedstock complexity and moving toward sugars, the amount of published work is scarce in the field of metal-based homogeneous catalysis. In this context, the aqueous phase reforming of glucose using homogeneous catalysts has been investigated using $[RuCl_2(p\text{-cymene})]_2$ in ionic liquids.[57] The authors suggested that the ionic liquids allowed for both catalyst and glucose dissolution, while the low hydrogen solubility hindered hydrogen-consuming side reactions. NMR analyses on reaction mixtures showed that glucose was hydrated to HMF and transformed into levulinic and formic acid, with the latter responsible for hydrogen production by further conversion to H_2 and CO_2. Finally, the catalytic system proposed was also active in the conversion of pure cellulose with H_2 yields of up to 31% and 12% for glucose and cellulose respectively. However, the need of using ionic liquids and their complex purification and regeneration from reaction products may hinder the applicability of this process. Other authors employed different water-soluble homogeneous Ru complexes (best one $[(p\text{-cymene})Ru(NH_3)Cl_2]$) to produce hydrogen from glucose at a relatively low temperature (98°C).[58] From the liquid phase analysis the authors suggested that the hydrogen formation could be derived from formic acid decomposition or from the "aldehyde water shift reaction",[59,60] where the terminal aldehyde was oxidised to carboxylic acid, releasing one molecule of H_2. Further C-C cleavage would have led to formic acid production, although this has not been fully investigated. The catalyst activity was correlated to the acidity - as a free proton was needed to close the cycle - and the best results were obtained at a pH=0.5, condition that hindered further possible applications due to high corrosivity. Ir and Ru PNN and PNP pincer catalysts were also employed in the aqueous phase reforming of sugars: the authors screened different substrates such as fructose, glucose, cellobiose, hydrolysed cellulose and lignin, showing outperformance of Ir if compared to Ru.[61] Unfortunately, the reaction mechanism was not identified as only the gas phase was analysed.

Compared to other Ru-based homogeneous catalysts, some advantages could be provided using cyclopentadienone ruthenium molecular pre-catalysts.[62,63] Among others, the commercial Shvo complex, never employed in molecular hydrogen production from sugars, could match a high stability

as a pre-catalyst and an easy synthesis and handling.[64,65,66] It generally well performed also in complex reaction mixtures in the absence of acidic and basic additives, as previously demonstrated by our research group. Shvo complex was used in the upgrading of bio-oils and in the reduction of biomass derived feedstocks, showing interesting performances both in hydrogenation, H-transfer and depolymerization of sugar oligomers.[67,68]

In this work we investigated the aqueous phase reforming of glucose using homogenous Ru-based cyclopentadienone complexes in order to investigate their activity in hydrogen production from renewable feedstocks. Different substrates, catalysts, reaction conditions and additives were screened as well as the use of an ionic liquid as a co-solvent. Moreover, *in situ* NMR analysis was employed to shine a light on the reaction mechanism involved in the hydrogen production process from glucose. As previously mentioned, hydrogen could be generated from the aldehyde water shift mechanism or by formic acid obtained by C-C cleavage, or from its coproduction with levulinic acid.[58] The discrimination between the two possible reaction mechanisms can help to build future catalytic systems with higher activity.

Results and discussion

Shvo-type cyclopentadienone complexes reported in chart 1 were selected as promising candidates for the production of hydrogen by aqueous phase reforming and were tested as pre-catalysts for the hydrogen evolution from glucose under the following conditions: dimethylsulfoxide (DMSO)/H_2O 1:1, T = 150°C, t = 4h, [cat] = 2 mol%. The catalysts were inactive at lower temperatures.
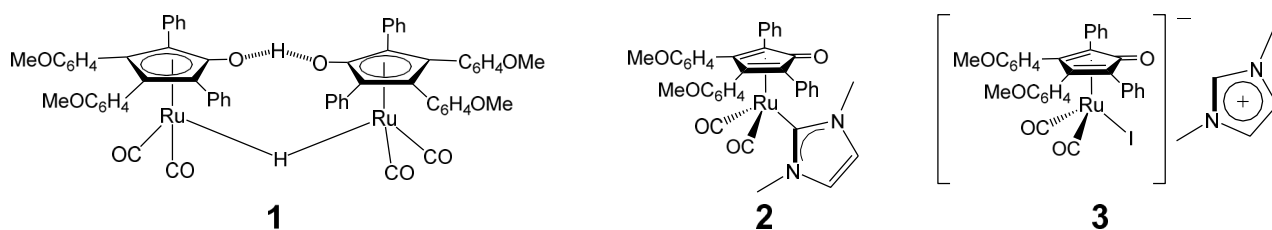
Chart 1. Complexes employed as pre-catalysts in this work.

Shvo complex **1** is largely employed in hydrogen borrowing applications and resulted to be active in both hydrogenation and dehydrogenation reactions.[65,66] Complex **2**, which has lower activity in hydrogenation, could be more prone to dehydrogenation, upon activation thanks to the releasing of a CO group, due to the presence of a stable sigma donor ligand such as a N-heterocyclic carbene.[69] Complex **3** is a largely stable complex that can be activated in the same form as the Shvo precursor with improved solubility in polar solvents, such as ionic liquids.

The obtained results, reported in Table 1, showed that the best performance in terms of hydrogen production was achieved with Shvo catalyst **1** (entry 1, glucose conversion = 15.2%). Although at this temperature all the catalysts should have been activated, this behavior could be ascribed both to the easier activation of Shvo complex **1** in comparison with **2**[70,71,72] and **3**,[63] and to its higher efficiency in transfer hydrogenation (*vide infra*).

Table 1. Gaseous hydrogen yield in APR reaction of glucose catalyzed by different catalysts (2 mol%) at 150 °C in DMSO/H_2O 1:1 after 4 hours.

Entry	Substrate	Catalyst	H_2 Yield (%)
1	Glucose	**1**	19.1
2	Glucose	**2**	2.0
3	Glucose	**3**	4.8

On these basis, Shvo catalyst **1** has been selected for the following condition screenings. To analyze the activity of the complex towards biomass-derived sugars and polyols which could be reactive under APR conditions, the process was tested with fructose, arabinose, sorbitol, and glycerol as substrates. The reactions were carried out at 150°C for 4 hours in a DMSO/H_2O 1:1 solution (catalyst loading 2 mol%; substrate concentration 0.166 mol/L) in order to favor the solubility of the catalyst. The results expressed as hydrogen yield are reported in Table 2. Blank tests, carried out feeding glucose and solvents or catalyst and solvents alone, showed negligible hydrogen formation, as expected.

Table 2. Gaseous hydrogen yield in APR reaction of sugars and polyols catalyzed by **1** (2 mol%) at 150 °C in DMSO/H_2O 1:1 after 4 hours.

Entry	Substrate	Catalyst	H_2 Yield (%)
1	Glucose	**1**	19.1
2	Fructose	**1**	0.4
3	Arabinose	**1**	14.6
4	Sorbitol	**1**	0.4
5	Glycerol	**1**	1.4

Among the screened sugars, reactions with glucose and arabinose led to hydrogen production, while no hydrogen was detected using fructose. No hydrogen evolution was also achieved in the aqueous phase reforming of polyols (sorbitol and glycerol). Accordingly, the structure and the functional groups of the biomass-derived compounds likely play a determining role in unlocking the hydrogen production pathways (*vide infra* for details on the proposed mechanism). Among the investigated substrates, the polyols are characterized by the presence of hydroxyl functional groups, while sugars bear a C=O bond in their open-chain structure. In particular, the ketonic group in fructose is unreactive, while glucose and arabinose, displaying a terminal aldehyde could react with water in the "aldehyde water shift reaction" yielding a carboxylic acid and hydrogen, as reported by Goldberg et al.[73,74] (Scheme 1).
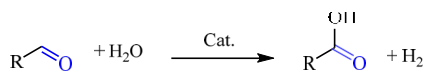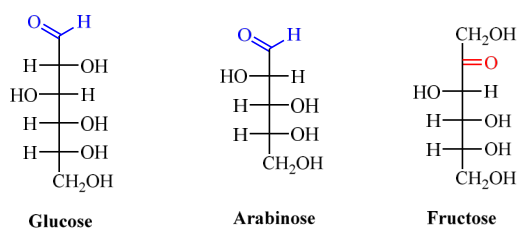
Scheme 1. Open chain form of glucose, arabinose, and fructose and aldehyde water shift reaction.

On the other hand, tests conducted using formic acid as substrate under the same reaction conditions provided an 88% hydrogen yield, suggesting that this compound is a plausible intermediate in the H_2-production process. Given the promising results obtained with glucose, this substrate was selected as reagent of choice for investigating the role of the catalyst and the reaction evolution in the APR process.

Mechanisms insights and analyses of the liquid phase

The crude mixtures (DMSO/H_2O) were extracted with dichlorometane (CH_2Cl_2) at the end of the reaction and analyzed by ^{1}H-NMR and FT-IR spectroscopy in order to monitor the presence of the catalyst and eventually of other derived organometallic species. From the organic fractions of the catalytic tests run in 1:1 DMSO/H_2O after 1 hour, it was possible to observe the typical Shvo's catalyst carbonylic stretching bands (2037, 2004 and 1987 cm^{-1}) (Figure S8). These signals were accompanied by less intense carbonylic stretchings at 2018 and 1960 cm^{-1} that were attributed to a mononuclear dicarbonyl ruthenium complex (*vide infra*). The unreacted Shvo's complex was also detected by ^{1}H-NMR analysis which displayed, among others, the signal corresponding to its typical bridging hydride at -18.5 ppm (Figure S1).[75]

Interestingly, in FT-IR analysis of the organic phases extracted after 4 hours of reaction, the complex **1** and the mononuclear ruthenium complex carbonylic stretching bands decreased in intensity, with new signals arising at 1946 and 1921 cm^{-1} (Figure S10). Also, from NMR spectrum the Shvo's

hydride signal was replaced by two new ruthenium terminal hydrides at -13.1 and -14.3 ppm (Figure S2).[44] Although it was not possible to precisely assign the new signals to ruthenium complexes due to their low stability, the resting state mixture analysis indicated that the catalyst was probably prone to deactivation at longer reaction times. In general, no traces of organic compounds were visible in the above-mentioned spectrum, confirming that the organic extractions did not interfere with the analysis of the aqueous phase (Figure S1).

Luckily by performing the reaction in only water it was possible to evaluate the process at the intermediate level. In this case indeed, the FT-IR analysis on the extracted organic phase after 4h, revealed that Shvo's catalyst **1** stretching bands were no more visible, while only the bands at 2018 and 1961 cm^{-1} were detected (Figure S12). As already stated, this shift is compatible with the formation of a monomeric ruthenium species containing two terminal carbonyl groups, with a higher metal carbonyl backbonding electron donation. In this way, a sigma bonding ligand on the vacant site of ruthenium could be expected. The identity of this new ruthenium complex was investigated by ^{1}H-NMR spectroscopy and ESI-MS. In particular, the ^{1}H-NMR spectrum displayed the presence of an aldehyde at 9.62 ppm but no hydride signals were visible (Figure S3).

On the other hand, ESI-MS analysis gave some hints on the plausible formation of a species with m/z 728+1 [M+1]$^+$ (Figure S13), in accordance with the monomeric structure **4** reported in Figure 1.
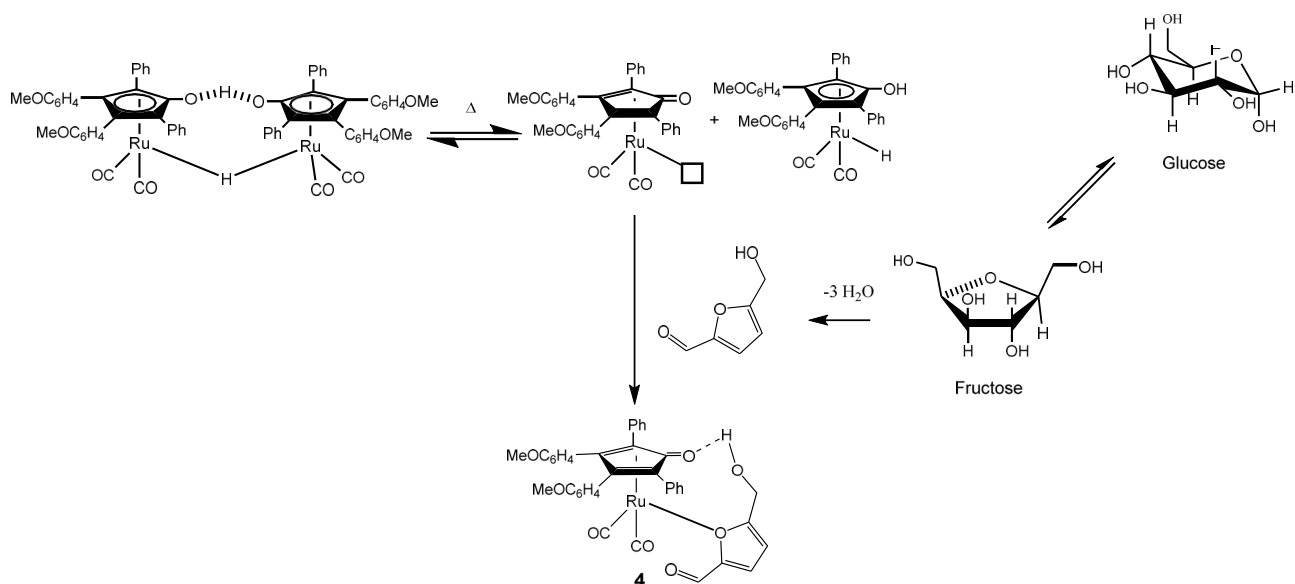
Figure 1. Proposed catalyst stabilization in the reaction resting state.

It is well known that 5-hydroxymethylfurfural (HMF) can be obtained by the dehydration of fructose after isomerization of glucose at high temperatures.[76,77] Furthermore, similar interactions were supported by DFT calculations between the activated Shvo's catalyst **1** and 2,5-dihydroxymethylfuran (BHMF), as reported by our group in a previous paper.[67]

This phenomenon could also justify the lower activation of fructose (0.4% H_2 yield) if compared with glucose (19.1% H_2 yield) under the same reaction conditions (see Table 2, entries 1 and 2).

To identify products derived from glucose transformation, the APR process was also monitored by ^{1}H-NMR *in situ,* without working-up the final resulting mixtures (see Experimental), confirming the formation of HMF (δ 9.36 ppm: HMF aldehyde; δ 7.41, 6.53 ppm: HMF furanic protons), as highlighted in Figure 2.
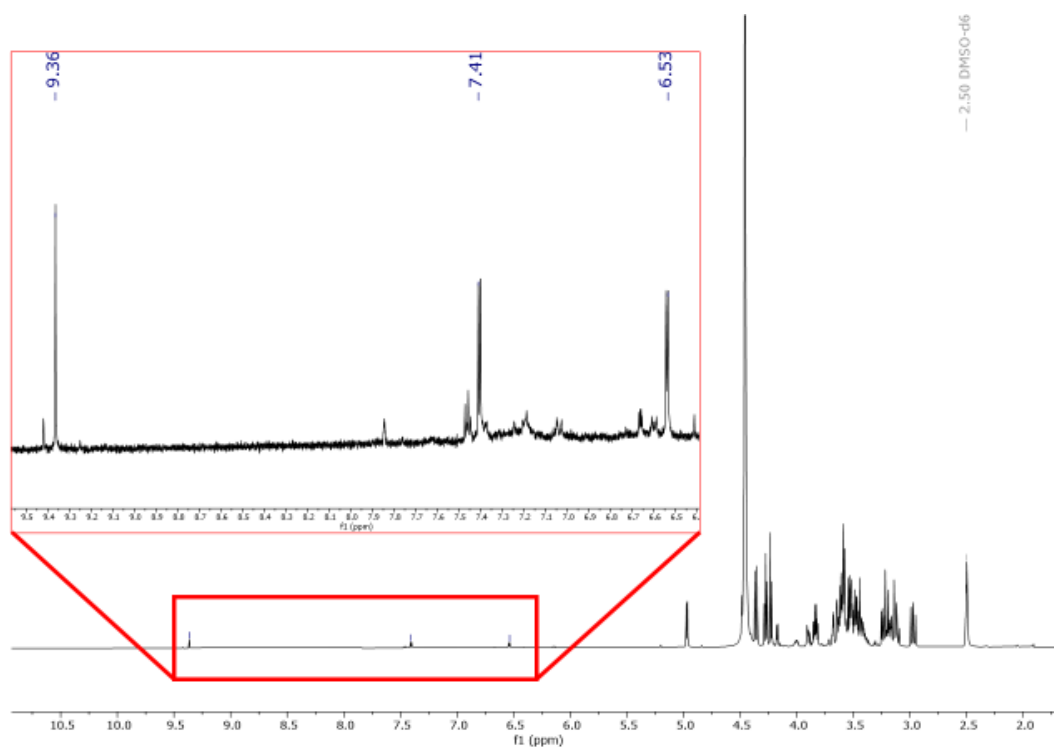
Figure 2. *In situ* ^{1}H-NMR spectrum of APR reaction conditions: DMSO d_6/D_2O 1:1 solution, 2 mol% **1**, 4h, 150°C. Aldehyde region is enlarged.

The reaction course over time also revealed new signals in the 3.5-4.5 ppm region due to the anomerization of glucose (Figure 3).
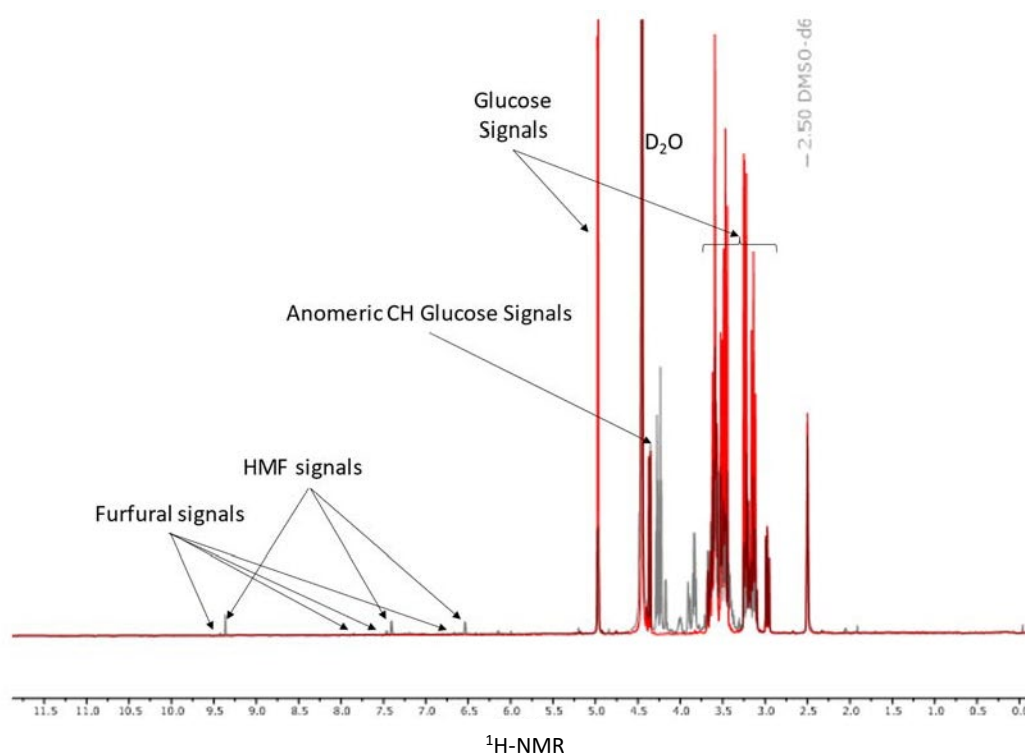
Figure 3. *In situ* ^{1}H-NMR spectrum of glucose APR reaction. Comparison between monitoring at 1h (red) and 4 hours (dark grey). Conditions: DMSO d_6/D_2O 1:1 solution, 2 mol% **1**, 150°C.

Since arabinose was also found to be active in the Shvo-catalyzed H_2 production (Table 2), we wondered if it could be part of the reaction as an intermediate substrate due to the transformation of glucose to arabinose.[58] This reaction is accompanied by the co-formation of formic acid that could be easily reformed to CO_2 and hydrogen by catalyst **1** as above described. Another way in which carbon dioxide could be formed is the water gas shift reaction (eq. 3) occurring over carbon monoxide that can be formed in reforming reactions.[78,79] However, according to the reaction mechanism proposed here and validated by NMR analysis, glucose decomposition over Shvo does not involve the decarbonylation of the substrate to give CO, while formic acid decomposition is responsible for direct CO_2 production. With the aim of detecting arabinose reforming products, APR was directly conducted using arabinose as a substrate in a J-Young's tap NMR tube for an *in-situ* monitoring (DMSO d_6 - D_2O 1:1 solvent mixture, 2 mol% **1**, 4h, 150°C). At the end of the reaction, the formation of furfural (aldehydic proton at δ 9.41 ppm and furanic ring protons at δ 7.48, 7.45, 6.66 ppm) was clearly observed (Figure 4). Since furfural, derived from arabinose dehydrogenation, was detected

also in the more complex reaction mixture derived from glucose APR, the step of glucose transformation to arabinose under reforming conditions was confirmed.
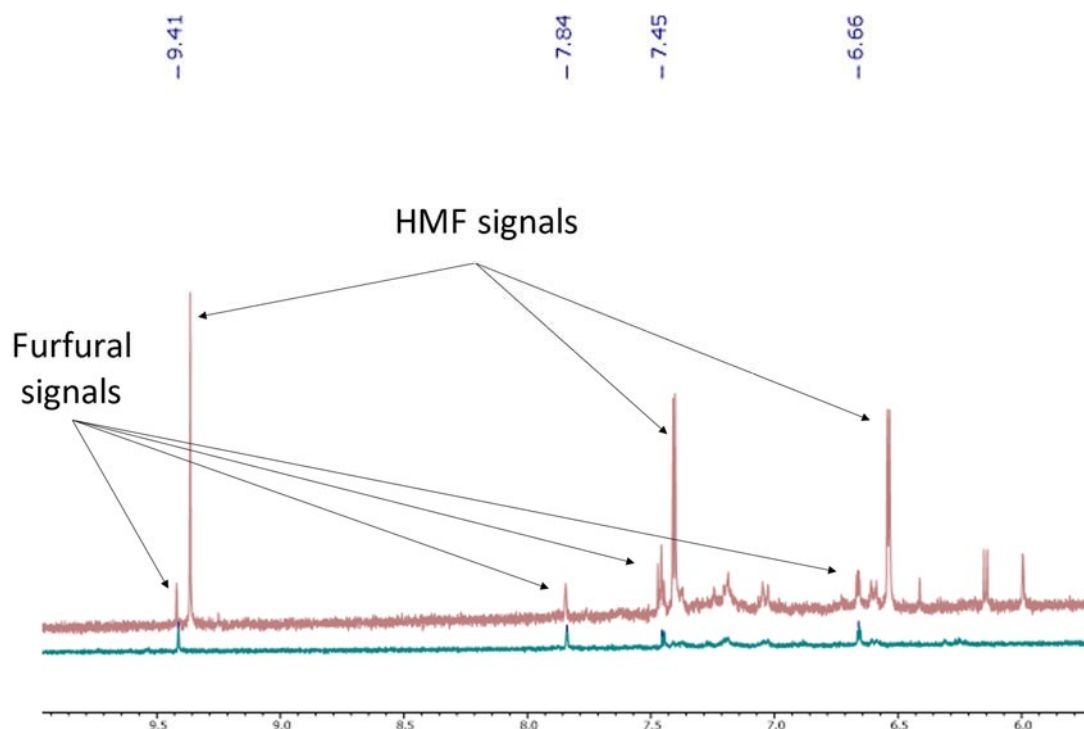
Figure 4. *In situ* ^{1}H-NMR spectrum APR reaction of glucose (in red) and arabinose (in blue), enlargement of aldehydes and furan region. Conditions: DMSO d$_6$/D$_2$O 1:1 solution, 2 mol% **1**, 150°C.

Unfortunately, no other products deriving from arabinose could be assigned due to their low concentration and to the complexity of the ^{1}H-NMR spectrum. However, we could also hypothesize some hydrogen production deriving from the decarboxylation of arabinose to erythrose, according to the proposed mechanism for glucose transformation under APR conditions as depicted in Scheme 2.
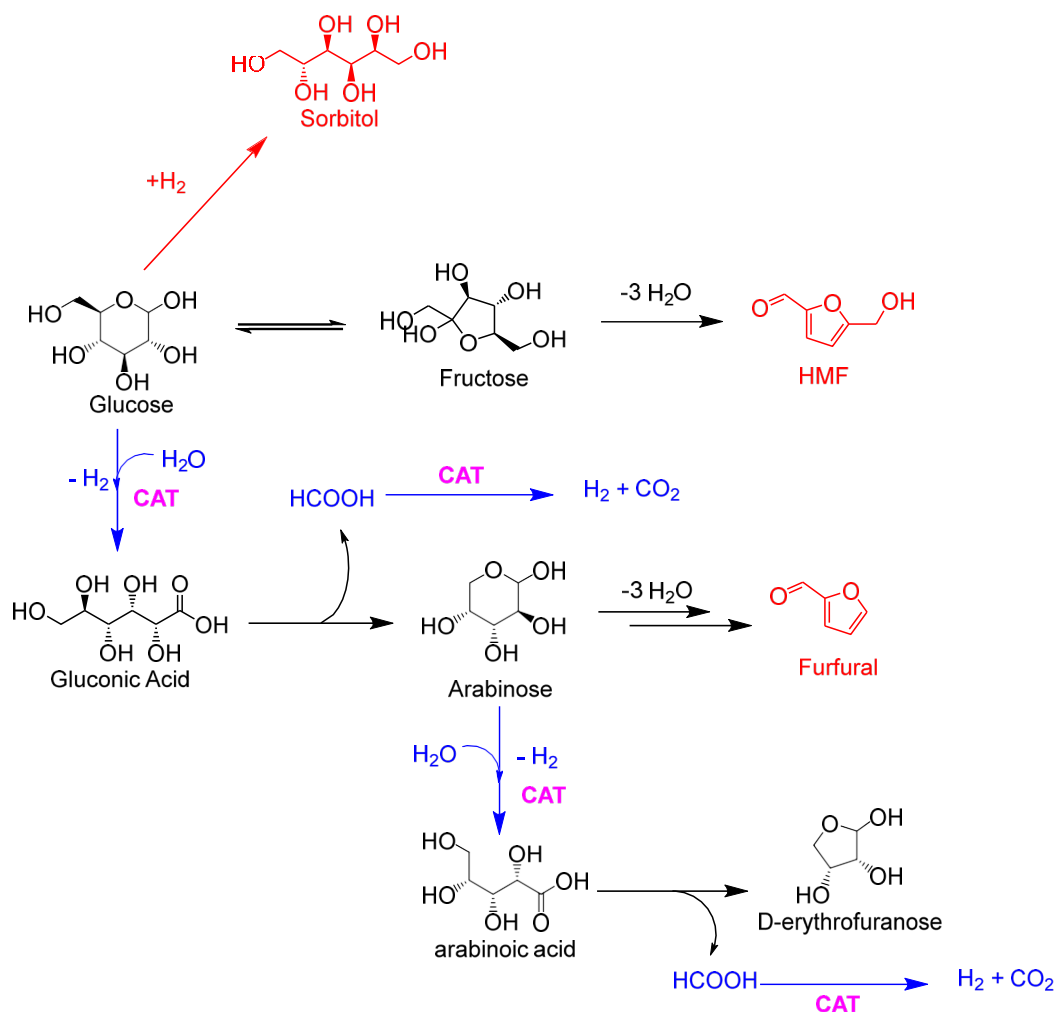
Scheme 2. Proposed mechanism for the homogeneously catalyzed APR process of glucose.

To shine a light on the co-formation of products or partially oxidized carbohydrates, the liquid phases of a batch reaction were also analysed by HPLC chromatographic analysis. After the reactions, the catalyst was removed from the system through washings with CH_2Cl_2, and the resulting cloudy aqueous phase was filtered and injected in HPLC. All the chromatograms revealed the presence of glucose, sorbitol and fructose as the only components of the mixture. The filtered residue revealed the formation, although scarce, of insoluble humins from carbohydrates condensation.[80]

As reported in Scheme 2, sorbitol is the hydrogenated product of glucose, suggesting that the catalyst was able to transfer the hydrogen produced by glucose to another molecule of substrate. Although this subsequent reaction did not contribute to the total gas yield, a higher efficiency of the Shvo catalyst in the dehydrogenation of glucose was demonstrated.

Monitoring the glucose APR reaction over time (Table 3), the best conditions were found at 2.5 hours, where the H_2 production resulted 28.9 % (entry 3), TON = 15. These results candidated Shvo's complex as a competitive pre-catalyst for APR in comparison with molecular catalysts available in the state of the art and discussed in the introduction.

Table 3. Gaseous hydrogen, fructose and sorbitol yield over time in APR reaction of glucose catalyzed by **1** (2 mol%) at 150 °C in DMSO/H_2O 1:1.

Entry	Substrate	Catalyst	Time (h)	H_2 Yield (%)	Conversion (%)	Fructose Yield (%)	Sorbitol Yield (%)
1	Glucose	**1**	0.5	0.3	1.8	0.8	-
2	Glucose	**1**	1	8.4	4.3	0.9	0.8
3	Glucose	**1**	2.5	28.9	11.4	0.9	1.8
4	Glucose	**1**	4	19.1	15.2	3.3	6.1

In general, negligible or low hydrogen production was observed at low reaction times (entry 1 and 2), likely due to an induction time that is needed for the activation. Moreover, in almost all the cases, glucose conversion resulted lower than H_2 yield (entries 2-4), suggesting the occurrence of subsequent dehydrogenation reactions on intermediates as depicted in Scheme 2. Reached the maximum hydrogen yield at 2.5 hours (28.9%), the latter decreased to 19.1% after 4 h (entry 4). Concurrently sorbitol, the product expected from glucose hydrogenation, increased with time, reaching a maximum at 4 h (yield 6.1%, entry 4). A reasonable explanation of these peculiar behavior resides in the acknowledged high efficiency of the Shvo complex as a polar double bond hydrogenation catalyst[64-66] that could reduce glucose, HMF, furfural (detected by *in situ* NMR) or other co-products, causing molecular hydrogen yield depletion.[67] Glucose conversion needs also to take account of the formation of a small amount of fructose (see entry 4 and Scheme 2).

Inspired by our precedent work,[44] 1,4-benzoquinone (BQ) was added to the reaction to promote catalyst dehydrogenation. This electron transfer mediator was found to behave as a hydrogen acceptor from the reduced catalyst, promoting further dehydrogenation of the substrate and favoring the overall

conversion. We evaluated different amounts of the additive in the reaction (benzoquinone 2, 10, 20 mol%), as reported in Table 4.

Table 4. Gaseous hydrogen, fructose and sorbitol yields in APR reaction of glucose catalyzed by different catalysts (2 mol%) with BQ as additive at 150 °C in DMSO/H_2O 1:1 after 4 hours.

Entry	Substrate	Catalyst	BQ (mol%)	H_2 Yield (%)	Conversion (%)	Fructose Yield (%)	Sorbitol Yield (%)
1	Glucose	**1**	2	23.2	20.9	3.5	6.3
2	Glucose	**1**	10	14.9	17.8	2.9	6.0
3	Glucose	**1**	20	14.4	14.8	2.2	6.1
4	Glucose	**2**	2	6.18	19.2	5.9	6.2
5	Glucose	**3**	2	17.7	16.6	4.0	5.0

An equimolar additive/catalyst **1** amount slightly affected the hydrogen production (from 19.1% entry 4, table 3 to 23.2% cat **1**, 2 mol% BQ, entry 1) and glucose conversion (from 15.4% entry 4, table 3 to 20.9% entry 1). On the other hand, when the additive was increased, a reduction in molecular hydrogen yield was detected (entries 2 and 3), highlighting a role of BQ as hydrogen acceptor toward the formation of stable hydroquinone (Scheme 3). Nevertheless, the effect of BQ on glucose conversion is not trivial due to the lack of a complete carbon balance and to the complexity of the equilibria involved in the reaction as previously stated (Scheme 2).
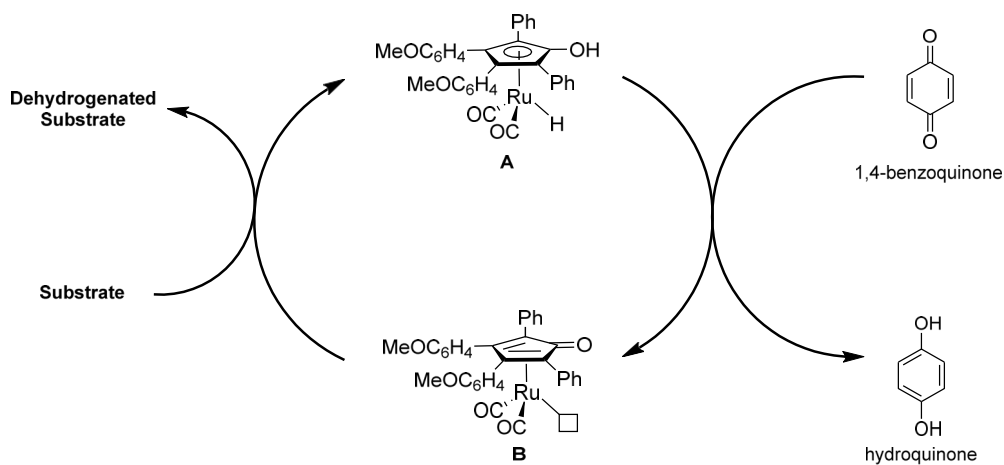
Scheme 3. Role of BQ in the dehydrogenation of glucose catalyzed by Shvo complex **1**.

Surprisingly, BQ was prone to favor the activation of the less promising complexes **2** and **3** (entries 4 and 5). Its positive effect was in fact even more visible when the protocol was applied to less reactive catalysts (**2**: 2%, entry 2, Table 1 vs. 6.18% with 2 mol% BQ, entry 4; **3**: 4.8%, entry 3, Table 1 vs 17.7% with 2 mol% BQ). Sorbitol yields were not affected by the additive, while in the case of **2** and **3**, fructose formation increased, in line with an expected higher induction time for the catalyst activation. This was likely to also affect glucose conversion, which even in these cases was not easy to be correlated to yields due to lack of complete carbon balance. In general, better results were observed with a lower BQ loading, which could help the catalyst activation toward dehydrogenation. The effect of the pH on hydrogen production was generally reported as affecting homogeneous catalysts efficiency under APR conditions.[58,61] Moreover, a higher pH could favor carbohydrate dissolution and degradation to simpler molecules via retro-aldol reactions.[81,82]

When a variation of the pH reaction mixture was attempted in the standard protocol with catalyst **1**, a decrease in the total hydrogen yield was observed both in acidic (2 mol% **1** at 150 °C, 4h, pH 4 (H_2SO_4), H_2 yield 16.4%) and basic solutions (2 mol% **1** at 150 °C, 4h, pH 10 (NaOH), H_2 yield 17.2%), with neutral conditions confirming as the best. In fact, Shvo catalyst is used to be active without the need for an acid/base additive.[65,66] From a mere acid/base point of view, an acidic medium is likely to protonate the cyclopentadienone of intermediate **B** (Scheme 3) leading to a less active form of the catalyst.[70] Catalyst dehydrogenation performances can also be affected by the base which is prone to deprotonate the hydroxycyclopentadienyl in the **A** form (Scheme 3), affecting hydrogen evolution or H-transfer reaction with a detrimental effect on the overall catalytic performance. On the other hand, the base can also coordinate to the ruthenium center influencing the reaction kinetic.

A last exploration was performed to test the catalyst performance in ionic liquids, which are increasing their importance as solvents in many fields, and have been successfully applied in aqueous reforming of carbohydrates.[57,58] Their relevance arises in their easy dissolution capability of different

carbohydrates and more importantly, low hydrogen solubility, which could thus ideally limit the re-hydrogenation of glucose to sorbitol.

In this context, we selected 1-butyl-3-methylimidazolium trifluoromethanesulfonate (Bmim[TfO]) due to its ready availability, for being tested in the standard protocol of glucose APR (Bmim[TfO]/H$_2$O 1:1, T= 150 °C, 4h, **1** 2 mol%). Unfortunately, under these conditions the gaseous H$_2$ production was almost negligible (1.3%). We hypothesized that Shvo's complex could undergo deactivation via the formation of a ruthenium cyclopentadienone ionic pair complex similar to **3** (Chart 1 and Table 1) that revealed low catalytic activity (H$_2$ yield 4.8% in DMSO/H$_2$O mixture 1:1) in this reaction. The excess of imidazolium salt was likely to favor the complete deactivation of **1** as depicted in Scheme 4. Although OTf$^-$ is a less coordinating anion if compared with iodide (anionic ligand in **3**), triflate has been previously found to coordinate the ruthenium center in this kind of reactivity.[63]
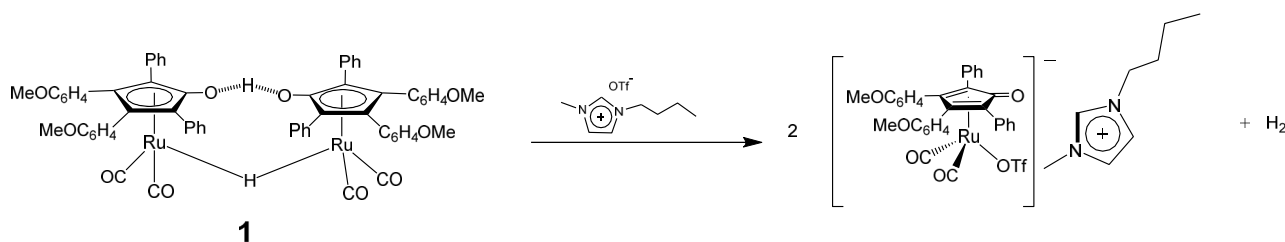
Scheme 4. Proposed deactivation of Shvo catalyst **1** in ionic liquid Bmim[TfO].

Conclusions

Cyclopentadienone ruthenium complexes **1**, **2** and **3** have been employed as molecular bifunctional catalysts in the homogeneous Aqueous Phase Reforming (APR) of glucose. The commercial Shvo's complex **1** resulted the most competitive among those investigated, with similar hydrogen production compared to other homogeneous catalysts reported in the literature. This catalyst also demonstrated to be prone to transfer the hydrogen produced during APR on glucose itself, toward the production of sorbitol and on other substrates suitable to be reduced. The use of acidic and basic additives was ineffective for the process, confirming that Shvo's complex outperformed in neutral medium. Adding

benzoquinone as an equimolar co-catalyst allowed the activation of pre-catalyst **2** and **3**. On the other hand, it displayed a detrimental effect if used in excess to the catalyst, probably due to the consumption of produced hydrogen in its reduction. The use of solvents such as imidazolium-based ionic liquids was prevented by the deactivation of the catalyst. *In situ* NMR and resting state studies allowed to identify the final fate of both the catalyst and the products, giving enlightening information on intermediates and the whole reaction pathway. Accordingly, these results could pave the way for the use of a class of bifunctional catalysts, bearing a cyclopentadienone moiety as a non-innocent ligand, which were by far underdeveloped but resulted very promising in hydrogen production from biomass derivatives.

Experimental section

Dichloromethane (CH_2Cl_2), dimethylsulfoxide (DMSO), distilled water, 1-butyl-3-methylimidazolium trifluoromethanesulfonate, $CDCl_3$ (Alfa Aesar) were used without additional purification. Sodium hydroxide (NaOH), Sulfuric Acid, Glucose, Sorbitol, Fructose, Arabinose, Formic Acid, Glicerol (Sigma Aldrich) were used as purchased. Shvo's complex,[76] dicarbonyl(η^4-3,4-bis(4-methoxyphenyl)-2,5-diphenylcyclopenta-2,4-dienone)(1,3-dimethylimidazol-2-ylidene)ruthenium (**2**),[62] Dicarbonyl(η^4-3,4-bis(4-methoxyphenyl)-2,5-diphenylcyclopenta-2,4-dienone)(iodine)ruthenium [1,3-dimethylimidazolium] (**3**), [43] were prepared as previously reported. p-benzoquinone (Alfa Aesar) was purified by column chromatography (stationary phase: silica gel, eluent: CH_2Cl_2).

NMR spectra were acquired at 298 K with a Varian Mercury Plus VX 400 (1H, 399.9; 13C, 100.6 MHz), or a Varian Inova 600 (^{1}H, 599.7; ^{13}C, 150.8 MHz) spectrometers. Chemical shifts were internally referenced to residual solvent peaks. Full ^{1}H- and ^{13}C-NMR assignments were accomplished, if necessary, with the aid of gHSQC and gHMBC NMR experiments using standard Varian pulse sequences. Infrared spectra were acquired at 298 K on a Perkin-Elmer Spectrum 2000 FT-IR spectrophotometer. ESI-MS spectra were obtained by dissolving samples in MeOH or CH_3CN and injecting the resulting solution into a Waters Micromass ZQ 4000.

Gas analyses were carried out off-line in a Thermo Focus GC with a CARBOSPHERE 80/100 6 × 1/8 column and a Thermal Conductivity Detector (TCD detector). Liquid products were analyzed with an Agilent HPLC over Rezex ROA Organic Acid column (0.0025 M H_2SO_4 mobile phase at 30 or 60 °C and a flux of 0.6 mL/min) with Diode-Array Detector (DAD) and Refractive Index Detector (RID) detectors.

Glucose conversion, Sorbitol, fructose and hydrogen yield calculation

Glucose conversion, sorbitol, and fructose yields were determined by HPLC injections by means of calibration curves using xylitol as internal standard. (See formulae below)[17] The hydrogen gas was collected in a gas burette and then injected through a gas-tight syringe in GC -TCD; H_2 yield was calculated via a calibration curve using the ideal gas law. The yields of hydrogen are indicated as follows: 100% yield corresponds to the formation of 1 mol of hydrogen from 1 mol of glucose.[83]

$$Glucose\ Conversion\ (\%) = \frac{mol\ Glucose\ IN - mol\ Glucose\ OUT}{mol\ Glucose\ IN} \times 100$$

$$Sorbitol\ Yield\ (\%) = \frac{mol\ Sorbitol\ out}{mol\ Glucose\ IN} \times 100$$

$$Fructose\ Yield\ (\%) = \frac{mol\ Fructose\ out}{mol\ Glucose\ IN} \times 100$$

$$Hydrogen\ Yield\ (\%) = \frac{mol\ H_2\ out}{mol\ Glucose\ IN} \times 100$$

Substrate Aqueous Phase Reforming – General catalytic test

In a 10 mL J Young ampule, 0.006 mmol of ruthenium complex (0.02 eq.) and 0.333 mmol (1 eq.) of the chosen substrate were dissolved in a 1:1 DMSO/H_2O mixture under a nitrogen atmosphere. In selected entries benzoquinone (from 0.006 mmol to 0.06 mmol), NaOH (0.0002 mmol) or H_2SO_4 (0.0002 mmol) were added as additives in the reaction mixture Then, the reaction was stirred at 150°C from 30 minutes up to 4 hours. At the end of the reaction, the ampule was cooled down to room temperature and the pressure was measured through a gas burette. Gas aliquots (0.5 mL) were collected by a gas-tight Hamilton Syringe and analyzed by gas chromatography. The liquid phase was washed with 3 x 4 mL of CH_2Cl_2 and the resulting aqueous phase was diluted to 5 mL with

distilled water. The diluted aqueous solution was then passed through a filtering pad (0.45 micrometers) and analysed by HPLC chromatography according to the previously reported method.[25] The organic phases arising from CH_2Cl_2 washings were analyzed by NMR and IR in order to verify the catalyst's fate at the end of the reaction.

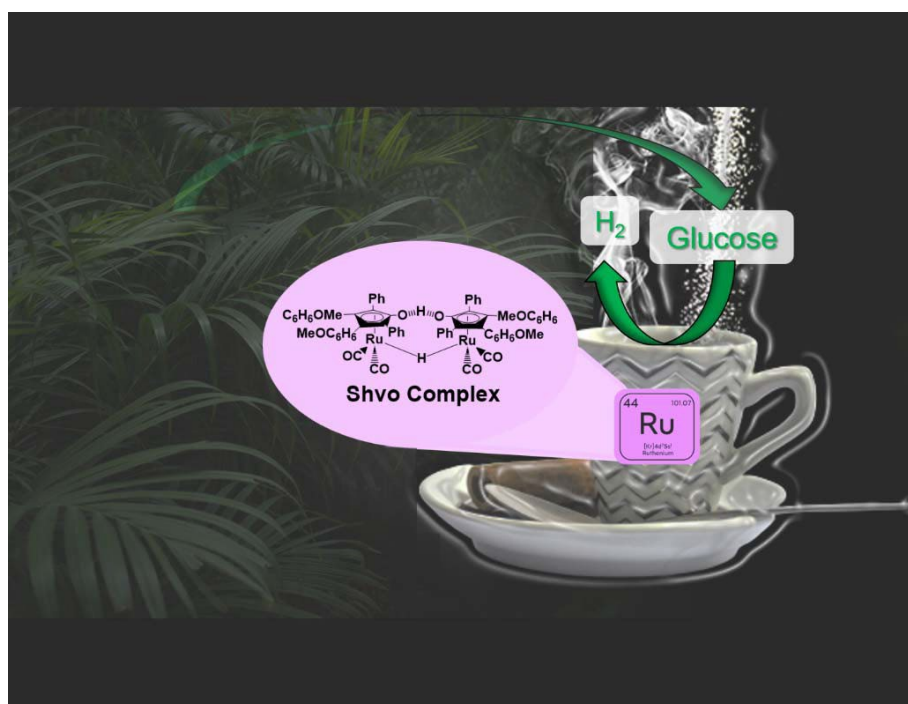**Substrate Aqueous Phase Reforming – General catalytic test in NMR tube**

In a J Young's tap NMR tube, 4 mmol of Shvo's complex (0.02 eq.) and 0.166 mmol (1 eq.) of the chosen substrate was dissolved in a 1:1 DMSO d_6/D_2O mixture under a nitrogen atmosphere, stirred at 150°C. Then, the mixture was cooled down to room temperature and analyzed by ^{1}H-NMR spectroscopy after 1 and 4 hours of reaction.

Supporting information

Supporting information: NMR spectra, ESI-MS and GC analyses are available at …

Table of contents

Ruthenium cyclopentadienone homogeneous bifunctional complexes and in particular Shvo's catalyst are suitable for the production of gaseous hydrogen from glucose under Aqueous Phase Reforming (APR) conditions.

References

[1] A. Pareek, R. Dom, J. Gupta, J. Chandran, V. Adepu, P.H. Borse, *Mat. Sci. Ener. Tec.* **2020**, *3*, 319–327.

[2] H. Council, **2017**. https://www.h2knowledgecentre.com/content/policypaper1203.

[3] HJ, Energy - European Commission, **2019**, https://energy.ec.europa.eu/topics/energy-systems-integration/hydrogen_en.

[4] IEA (2022), Hydrogen Supply, IEA, Paris https://www.iea.org/reports/hydrogen-supply, License: CC BY 4.0.

[5] R.R. Davda, J.W. Shabaker, G.W. Huber, R.D. Cortright, J.A. Dumesic, *Appl. Cat. B: Env.* **2003**, *43*, 13–26.

[6] R.R. Davda, J.W. Shabaker, G.W. Huber, R.D. Cortright, J.A. Dumesic, *Appl. Cat. B: Env.* **2005**, 56, 171–186.

[7] G.W. Huber, R.D. Cortright, J.A. Dumesic, *Angew. Chem.* **2004**, *116*, 1575–1577.

[8] R. R. Davda, J. A. Dumesic, *Chem. Comm.* **2004**, 36–37.

[9] J.W. Shabaker, R.R. Davda, G.W. Huber, R.D. Cortright, J.A. Dumesic, *J. Catal.* **2003**, *215*, 344–352.

[10] A. Fasolini, D. Cespi, T. Tabanelli, R. Cucciniello, F. Cavani, *Catalysts* **2019**, *9*, 722.

[11] A. Fasolini, R. Cucciniello, E. Paone, F. Mauriello, T. Tabanelli, *Catalysts* **2019**, *9*, 917.

[12] P.D. Vaidya, J.A. Lopez-Sanchez, *Chem. Select* **2017**, *2*, 6563–6576.

[13] P.D. Vaidya, A.E. Rodrigues, *Chem. Eng. Technol.* **2009**, *32*, 1463–1469.

[14] W.-H. Chen, C.-Y. Chen, Applied Energy **2020**, *258*, 114078.

[15] A. Fasolini, E. Lombardi, T. Tabanelli, F. Basile, *Nanomaterials* **2021**, *11*, 1175.

[16] A. Di Fraia, E. Miliotti, A.M. Rizzo, G. Zoppi, G. Pipitone, R. Pirone, L. Rosi, D. Chiaramonti, S. Bensaid, *AIChE Journal*, **2023**, *69*, e17652.

[17] G. Pipitone, G. Zoppi, A. Frattini, S. Bocchini, R. Pirone, S. Bensaid, *Catal. Today* **2020**, *345*, 267–279.

[18] E. Tito, G. Zoppi, G. Pipitone, E. Miliotti, A.D. Fraia, A.M. Rizzo, R. Pirone, D. Chiaramonti, S. Bensaid, *J.Env. Chem. Eng.* **2023**, *11*, 109076.

[19] G. Pipitone, G. Zoppi, R. Pirone, S. Bensaid, *Int. J. Hydrogen Energy* **2022**, *47*, 151–180.

[20] N. Di Fidio, S. Fulignati, I. De Bari, C. Antonetti, A.M. Raspolli Galletti, *Biores. Tech.* **2020**, *313*, 123650.

[21] C. Antonetti, A.M. Raspolli Galletti, D. Licursi, S. Fulignati, N. Di Fidio, F. Zanetti, A. Monti, T. Tabanelli, F. Cavani, *Catalysts* **2022**, *12,* 1189.

[22] G. Gliozzi, A. Innorta, A. Mancini, R. Bortolo, C. Perego, M. Ricci, F. Cavani, *Appl. Cat. B: Env.* **2014**, *145*, 24–33.

[23] M. Zeng, X. Pan, *Cat. Rev.* **2022**, *64*, 445–490.

[24] S.K.R. Patil, J. Heltzel, C.R.F. Lund, *Energy Fuels* **2012**, *26*, 5281–5293.

[25] S. Taghavi, E. Ghedini, F. Menegazzo, M. Signoretto, D. Gazzoli, D. Pietrogiacomi, A. Matayeva, A. Fasolini, A. Vaccari, F. Basile, G. Fornasari, *Processes* **2020**, *8*, 843.

[26] S.J. Dee, A.T. Bell, *ChemSusChem* **2011**, 4, 1166–1173.

[27] A. Messori, A. Fasolini, R. Mazzoni, *ChemSusChem* **2022**, 15, e202200228.

[28] G. Graziono, *Nat Rev Chem* **2018**, *2*, 1–1.

[29] K. Sordakis, C. Tang, L.K. Vogt, H. Junge, P.J. Dyson, M. Beller, G. Laurenczy, *Chem. Rev.* **2018**, 118, 372–433.

[30] Y. Zhao, K. Lu, H. Xu, L. Zhu, S. Wang, *Renew. Sust. Energy Rev.* **2021**, *139*, 110706.

[31] D. S. Morris, K. van Rees, M. Curcio, M. Cokoja, F. E. Kühn, F. Duarte, J. B. Love, *Catal. Sci. Technol.* **2017**,*7*, 5644-5649.

[32] J. R. Pankhurst, M. Curcio, S. Sproules, G. C. Lloyd-Jones, J. B. Love, *Inorg. Chem.* **2018**, *57*, 5915–5928.

[33] A. Messori, A. Gagliardi, C. Cesari, F. Calcagno, T. Tabanelli, F. Cavani, R. Mazzoni, *Catal. Today* **2023**, https://doi.org/10.1016/j.cattod.2023.01.010

[34] S. Werkmeister, J. Neumann, K. Junge, M. Beller, *Chem. –Eur. J.* **2015**, *21*, 12226–12250.

[35] T.D. Nixon, M.K. Whittlesey, J.M.J. Williams, *Dalton Trans.* **2009**, 753–762.

[36] D. Wang, D. Astruc, *Chem. Rev.* **2015**, *115*, 6621–6686.

[37] A. Nandakumar, S.P. Midya, V.G. Landge, E. Balaraman, *Angew. Chem. Int. Ed.* **2015**, *54*, 11022–11034.

[38] J. Campos, *Phys. Sci. Rev.* **2018**, 3.

[39] A. Dobson, S. D. Robinson, *J. Organomet. Chem.* **1975**, *87*, C52–3.

[40] D. Morton, D.J. Cole-Hamilton, I.D. Utuk, M. Paneque-Sosa, M. Lopez-Poveda, *J. Chem. Soc., Dalton Trans.* **1989**, 489–495.

[41] D. Morton, D.J. Cole-Hamilton, *J. Chem. Soc., Chem. Commun.* **1988**, 1154–1156.

[42] H. Junge, M. Beller, *Tetrahedron Letters* **2005**, *46*, 1031–1034.

[43] R. Mazzoni, C. Cesari, V. Zanotti, C. Lucarelli, T. Tabanelli, F. Puzzo, F. Passarini, E. Neri, G. Marani, R. Prati, F. Viganò, A. Conversano, F. Cavani, *ACS Sustain. Chem. Eng.* **2019**, 7, 224 – 237.

[44] C. Cristiana, A. Gagliardi, A. Messori, N. Monti, V. Zanotti, S. Zacchini, I. Rivalta, F. Calcagno, C. Lucarelli, T. Tabanelli, F. Cavani, R. Mazzoni, *J. Catal.* **2022**, *405*, 47 – 59.

[45] H. Junge, B. Loges, M. Beller, *Chem. Commun.* **2007**, 522–524.

[46] C. Gunanathan, D. Milstein, *Science* **2013**, *341*, 1229712.

[47] J. Choi, A. H. MacArthur, M. Brookhart, A. S. Goldman *Chem. Rec.* **2011**, *111*, 1761–79.

[48] H. Junge, B. Loges, M. Beller, *Chem Commun.* **2007**, 522–524.

[49] M. Nielsen, H. Junge, A. Kammer, M. Beller, *Angew Chem Int Ed.* **2012**, *51*, 5711–5713.

[50] D. Spasyuk, S. Smith, D. G. Gusev, *Angew Chem Int Ed.* **2012**, *51*, 2772–2275.

[51] D. Spasyuk, D. G. Gusev, *Organometallics* **2012**, *31*, 5239–5242.

[52] D. Morton, D. J. Cole-Hamilton, *J Chem Soc Chem Commun.* **1988**, 1154−1156.

[53] M. Nielsen, A. Kammer, D. Cozzula, H. Junge, S. Gladiali, M. Beller, *Angew. Chem. Int. Ed.* **2011**, 50, 9593−9597

[54] L. S. Sharninghausen, J. Campos, M. G. Manas, R. H. Crabtree, *Nat Commun.* **2014**, *5,*5084

[55] Z. Lu, I. Demianets, R. Hamze, N. J. Terrile, T. J. Williams, *ACS Catal.* **2016**, *6,* 2014−2017

[56] L. S. Sharninghausen, B. Q. Mercado, R. H. Crabtree, N. Hazari *Chem Commun.* **2015**, 51, 16201–16204.

[57] N. Taccardi, D. Assenbaum, M.E.M. Berger, A. Bösmann, F. Enzenberger, R. Wölfel, S. Neuendorf, V. Goeke, N. Schödel, H.-J. Maass, H. Kistenmacher, P. Wasserscheid, *Green Chem.* **2010**, *12*, 1150–1156.

[58] Y. Zhan, Y. Shen, S. Li, B Yue, X. Zhou, *Chem. Commun.*, **2017**,*53*, 4230-4233.

[59] S. Kar, J. Luo, M. Rauch, Y. Diskin-Posner, Y. Ben-David, D. Milstein *Green Chem.*, **2022**,*24*, 1481-1487.

[60] L. E. Heim, N. E. Schlörer, J.-H. Choi, M. H. G. Prechtl, *Nat Commun* **2014**, 5, 3621.

[61] Y. Li, P. Sponholz, M. Nielsen, H. Junge, M. Beller *ChemSusChem* **2015**, *8*, 804–808.

[62] C. Cesari, S. Conti, S. Zacchini, V. Zanotti, M.C. Cassani, R. Mazzoni, *Dalton Trans*, **2014**, *43*, 17240-17243.

[63] C. Cesari, A. Cingolani, M. Teti, A. Messori, S. Zacchini, V. Zanotti, R. Mazzoni, *Eur. J. Inorg. Chem.* **2020**, 1114 – 1122.

[64] M.C. Warner, C.P. Casey, J.E. Backvall, *Top Organomet. Chem.*, **2011**, *37*, 85-125.

[65] Y. Blum, Y. Shvo, *J. Organomet. Chem.* **1985**, *282*, C7–C10.

[66] B.L. Conley, M.K. Pennington-Boggio, E. Boz, T.J. Williams, *Chem. Rev.* **2010**, *110*, 2294-2312.

[67] T. Pasini, G. Solinas, V. Zanotti, S. Albonetti, F. Cavani, A. Vaccari, A. Mazzanti, S. Ranieri, R. Mazzoni, *Dalton Trans.* **2014**, *43*, 10224 – 10234.

[68] L. Busetto, D. Fabbri, R. Mazzoni, M. Salmi, C. Torri, V. Zanotti, *Fuel* **2011**, *90*, 1197 – 1207.

[69] C. Cesari, R. Mazzoni, E. Matteucci, A. Baschieri, L. Sambri, M. Mella, A. Tagliabue, F. L. Basile, C. Lucarelli, *Organometallics* **2019**, *38*, 1041–1051.

[70] C. Cesari, A. Cingolani, C. Parise, S. Zacchini, V. Zanotti, M. C. Cassani, R. Mazzoni, *RSC Adv.* **2015**, *5*, 94707 – 94718.

[71] C. Cesari, R. Mazzoni, H. Muller-Bunz, M. Albrecht, *J. Organomet. Chem.* **2015**, *793*, 256 – 262.

[72] C. Cesari, R. Conti, A. Cingolani, V. Zanotti, M. C. Cassani, L. Rigamonti, R. Mazzoni, *Catalysts*, **2020**, *10*, 264, 1 – 11.

[73] T. P. Brewster, W.C. Ou, J. C. Tran, K. I. Goldberg, S. K. Hanson, T. R. Cundari, D. M. Heinekey *ACS Catal.* **2014**, *4*, 3034–3038.

[74] A. S. Phearman, J. M. Moore, D. D. Bhagwandin, J. M. Goldberg, D. M. Heinekey, K. I. Goldberg, *Green Chem.*, **2021**, *23*, 1609-1615.

[75] C. Cesari, L. Sambri, S. Zacchini, V. Zanotti, R. Mazzoni, *Organometallics*, **2014**, *33*, 2814 – 2819.

[76] N. Taccardi, D. Assenbaum, M. E. M. Berger, A. Bösmann, F. Enzenberger, R. Wölfel, S. Neuendorf, Volker Goeke, N. Schödel, H. -J. Maass, H. Kistenmacherc, P. Wasserscheid, *Green Chem.*, **2010**, *12*, 1150-1156.

[77] K. Lourvanij, G. L. Rorrer, *J. Chem. Technol. Biotechnol.*, **1997**, *69*, 35–44.

[78] J. De Maron, R. Mafessanti, P. Gramazio, E. Orfei, A. Fasolini, F. Basile, *Nanomaterials*, **2023**, *13*, 53.

[79] A. Fasolini, R. Mafessanti, S. Abate, P. Gramazio, J. De Maron, G. Centi, F. Basile, *Cat. Today*, **2023**, *418*, 114047.

[80] R. Weingarten, A. Rodriguez-Beuerman, F. Cao, J. S. Luterbacher, D. M. Alonso, J. A. Dumesic, G. W. Huber, *Chemcatchem* **2014**, 6, 2229-2234.

[81] E. Alberico, P. Sponholz, C. Cordes, M. Nielsen, H.-J. Drexler, W. Baumann, H. Junge, M. Beller, *Angew. Chem. Int. Ed.* **2013**, *52*, 14162-14166.

[82] Y. Li, M. Nielsen, B. Li, P. H. Dixneuf, H. Junge, M. Beller *Green Chem.*, **2015**, *17*, 193-198

[83] G. Toyooka, T. Tanaka, K. Kitayama, N. Kobayashi, T. Watanabe , K.-i. Fujita *Catal. Sci. Technol.*, **2021**, *11*, 2273-2279